A COMPARISON BETWEEN CASCADED AND SINGLE-STAGE ORC SYSTEMS TAKEN FROM THE COMPONENT PERSPECTIVE

Martin T. White*, Matthew G. Read and Abdulnaser I. Sayma

Department of Mechanical Engineering and Aeronautics, City, University of London,
Northampton Square, London, EC1V 0HB, United Kingdom
E-mail: martin.white@city.ac.uk

* Corresponding author

ABSTRACT

Compared to single-stage ORC systems, cascaded ORC systems could have benefits for relatively high-temperature waste-heat recovery applications, which include the potential for higher expander isentropic efficiencies owing to lower expansion ratios, the removal of sub-atmospheric condensation pressures and the possibility to utilise two-phase expansion. Previous investigations suggest that cascaded systems could produce up to 5% more power than an equivalent single-stage system. The aim of this paper is to compare the different systems in terms of exergy destruction within the system and the heat-transfer area requirements. Firstly, the exergy analysis reveals that cascaded systems reduce the total exergy destruction related to the expansion process, but this is offset by the exergy destruction within the additional heat exchange process. However, cascaded cycles also lead to less exergy destruction within the heat-addition process. To assess the heat-transfer area requirements, a discretised double-pipe heat-exchanger model is developed for the condenser and intermediate heat exchanger that transfers heat from the topping cycle into the bottoming cycle, whilst a discretised finned-tube cross-flow heat-exchanger model is developed for the evaporator. The geometry of each heat exchanger is optimised to minimise the heat-transfer area subject to imposed pressure drop constraints. The results reveal that cascaded cycles require larger heat-transfer areas, which is due to the additional heat-transfer process and reduced temperature differences within the evaporator. Ultimately, the best performing cascaded cycles, which produce 4.0% and 5.9% more power than their single-stage counterparts, require 22.7% and 23.2% more heat-transfer area. Future investigations should investigate how this trade-off impacts economic performance.

1. INTRODUCTION

Organic Rankine cycle (ORC) systems are widely considered for the conversion of low-temperature heat, between around 80 and 400 °C, into power. However, at the higher end of this temperature range, ORC systems are associated with sub-atmospheric condensation pressures, leading to physically large condensers that need to operate under a vacuum, and large volumetric expansion ratios. For small-scale systems, large volumetric expansion ratios mean volumetric expanders are not suitable, whilst radial turbines can obtain the required expansion over a single stage, but are associated with increased secondary flows and clearance losses. Cascaded systems, in which a topping ORC feeds into a bottoming ORC (Figure 1), could have benefits compared to single-stage systems, including lower volumetric expansion ratios within each cycle and higher condensation pressures. The former could facilitate the design of more efficient expanders, whilst the latter could lead to more compact pipework and condensers as the potential for sub-atmospheric condensation pressures is removed. Moreover, reduced volumetric expansion ratios may introduce the possibility to achieve two-phase expansion using volumetric expanders, which could increase power output from waste-heat recovery systems (Read et al., 2017; Smith, 1993).

A few early studies demonstrated the potential of cascaded systems for low-temperature systems below 200 °C (Kane, 2003; Kosmadakis et al., 2009). More recently, the authors have conducted comparisons

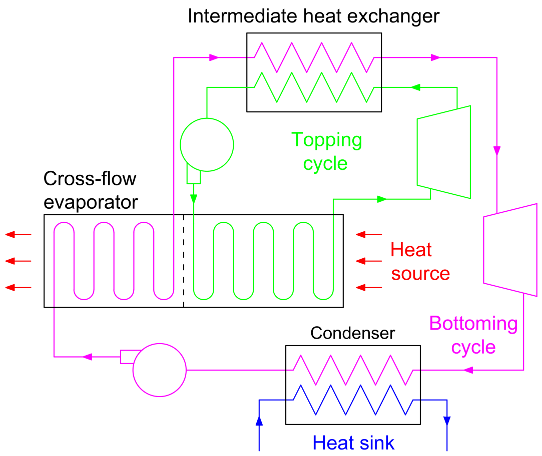

Figure 1: Schematic of the proposed cascaded ORC system.

of cascaded systems for higher temperature heat sources, operating with turbo- and twin-screw expanders with single- and two-phase expansion (White et al., 2018, 2019). These studies have suggested that cascaded systems, utilising two-phase expansion in the topping cycle, could produce up to 5% more power than an equivalent single-stage system. This comes at the cost of requiring additional components, but this could be offset by higher operating pressures that may reduce the required heat-transfer area.

The aim of this paper is to conduct a rigorous analysis to identify whether cascaded systems represent a better alternative to single-stage ORC systems for certain heat source conditions. This is conducted by firstly comparing the different systems in terms of thermodynamic performance and overall exergy destruction. Secondly, for each system, the design of each heat exchanger is optimised to identify optimal designs that meet both heat-transfer and pressure drop requirements. Thus, the results are helpful to identify whether cascaded cycles are a feasible alternative to single-stage systems.

2. THERMODYNAMIC ANALYSIS

In our previous study (White et al., 2019), three heat-sources, each assumed to be hot air with a mass-flow rate of 1 kg/s, were defined with temperatures of 473, 523 and 573 K. These temperatures are considered to represent temperatures where the choice between a single- or cascaded-system is unclear. The heat sink was water at a temperature of 15 °C with a mass-flow rate of 1 kg/s. The details of the thermodynamic analysis and optimisation can be found in White et al. (2018, 2019), which focussed on optimising single-stage and cascaded ORC systems to maximise the power output. Moreover, variable efficiency expander models were introduced to account for the effect of the volumetric expansion ratio on expander isentropic efficiency. The notation used to describe the considered cycles is given in Table 1. The 1-T and 1-S labels refer to single-stage systems operating with a turbine or screw expander respectively, whilst the 2-TT, 2-TS, 2-ST and 2-SS labels refer to cascaded systems where the first and second letters denote the expander type in the topping- and bottoming-cycle respectively. The maximum

Table 1: Summary of the six different cycles considered within this study.

Label	Type	Expander (top)	Expander (bottom)	Expansion (top)	Expansion (bottom)
1-T	single		turbine		single-phase
1-S	single		screw		single- or two-phase
2-TT	cascaded	turbine	turbine	single-phase	single-phase
2-TS	cascaded	turbine	screw	single-phase	single- or two-phase
2-ST	cascaded	screw	turbine	single- or two-phase	single-phase
2-SS	cascaded	screw	screw	single- or two-phase	single- or two-phase

Table 2: Summary of the optimal cycles identified for each cycle and heat-source temperature.

	T_{hi} = 473 K			T_{hi} = 523 K			T_{hi} = 573 K		
	$\dot{W}_n$	bottom	top	$\dot{W}_n$	bottom	top	$\dot{W}_n$	bottom	top
1-T	17.4	R245fa	–	27.3	pentane	–	38.2	cyclopentane	–
1-S	15.7	isopentane	–	24.3	R1233zd	–	32.6	cyclopentane	–
2-TT	16.7	isobutane	R1233zd	27.8	R1233zd	*n*-pentane	40.5	*n*-pentane	cyclopentane
2-TS	15.2	R245fa	R245fa	25.9	isopentane	*n*-pentane	38.4	*n*-pentane	cyclopentane
2-ST	17.2	isobutane	pentane	28.4	isopentane	benzene	40.4	cyclopentane	benzene
2-SS	16.2	isobutane	benzene	27.4	isopentane	benzene	38.6	cyclopentane	benzene

power output and optimal working fluids are summarised in Table 2. For the 573 K heat source, the 2-TT and 2-ST systems produce 6.1% and 5.9% more power than the 1-T system. For the 523 K heat source, the 2-ST system produces 4.0% more power than the 1-T system.

3. EXERGY ANALYSIS

For a given component, the exergy destroyed can be written as:

$$\dot{I} = \sum_{\text{in}} \dot{m}_{\text{in}} e_{\text{in}} - \sum_{\text{out}} \dot{m}_{\text{out}} e_{\text{out}} - \dot{W}, \tag{1}$$

where $\dot{m}_{\text{in}}$ and $\dot{m}_{\text{out}}$ are the mass-flow rates entering and leaving respectively, $\dot{W}$ is the work done, and e_{in} and e_{out} are the inlet and outlet specific exergy values. These are are calculated from:

$$e = (h - h_0) - T_0(s - s_0), \tag{2}$$

where h and s are the enthalpy and entropy of the fluid, and h_0 and s_0 are the enthalpy and entropy of the fluid at the dead state, defined by a temperature T_0 = 288 K and pressure P_0 = 101 kPa. A more detailed description of exergy analysis applied to ORC systems can be found in Lecompte et al. (2014).

The results from the exergy analysis are reported in Figure 2. In this figure, the results for the exergy destruction in the two pumps, two expanders and two heat-addition processes for the cascaded systems are grouped together to facilitate a comparison between the single-stage and cascaded systems. Unsurprisingly, there is a direct relationship between cycles that produce maximum power and those that result in the lowest exergy destruction. More interestingly, the combined exergy destruction for the two expansion processes within the cascaded cycles is lower than the single-stage systems. More specifically, for the 473, 523 and 573 K heat sources, the 2-TS, 2-TT and 2-TT systems correspond to 20.1%, 19.1% and 37.6% reductions respectively, compared to the 1-T systems. This is linked to lower volumetric expansion ratios, which lead to higher expander isentropic efficiencies. However, this reduction in exergy destruction is offset by the additional exergy destruction within the intermediate heat-exchange process. For the same three cascaded cycles, this exergy destruction is equal to 2.41, 1.21 and 2.27 kW respectively, which lead to net exergy destruction reductions of −0.01, −2.86 and −2.31 kW respectively for the combined effects of the increased expander efficiency and intermediate heat-exchanger process. The exergy destruction within the intermediate heat exchanger is low since both fluids undergo phase change, which allows a low temperature difference to be maintained for most of the heat exchange process.

For the optimal 523 and 573 K cascaded cycles (2-ST and 2-TT cycles respectively), the net exergy destruction rate for the combined expander and intermediate heat-exchange processes are +0.56 and −0.48 kW, compared to the 1-T systems. Comparatively, the net exergy destruction rates for the complete cycle are reduced by −1.14 and −1.53 kW. In both cascaded cycles exergy destruction within the pumps is greater than the 1-T systems. Thus, the heat-addition and heat-rejection processes are responsible for the remainder of the improved exergetic performance. This can be understood by considering the *T*-*s* diagrams for the 1-T and optimal cascaded systems (Figure 3). For the 523 K 2-ST cycle, two-phase

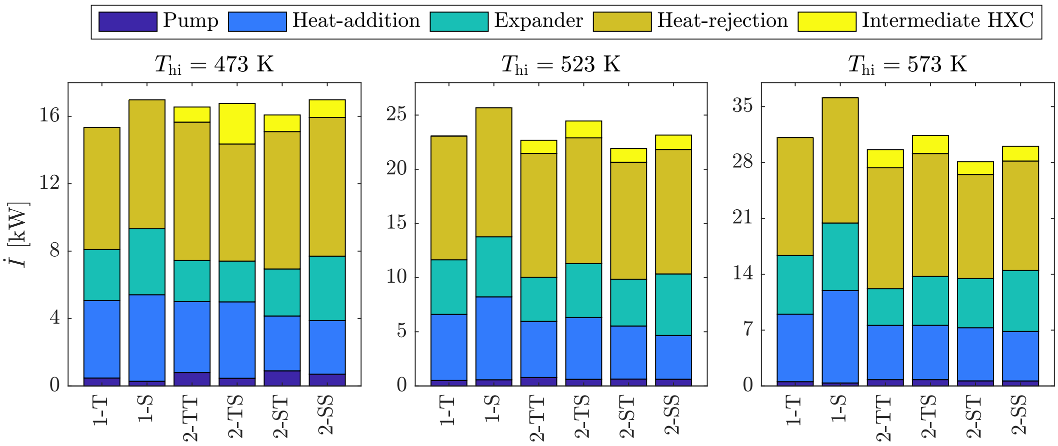

Figure 2: Comparison of the optimal cycles that maximise power generation for each cycle and heat-source temperature in terms of the exergy destruction within the cycle.

expansion in the topping cycle reduces exergy destruction within the topping-cycle evaporator as the isothermal heat-exchange process is partially removed. Moreover, since the expander outlet conditions in the topping cycle are two-phase, the bottoming cycle expansion starts from a saturated vapour state, which reduces the amount of superheat at the expander outlet, compared to the 1-T system, and reduces exergy destruction in the bottoming-cycle condenser. For the 573 K 2-TT system, the improved exergetic performance is the result of a reduction in the amount of heat transferred during evaporation.

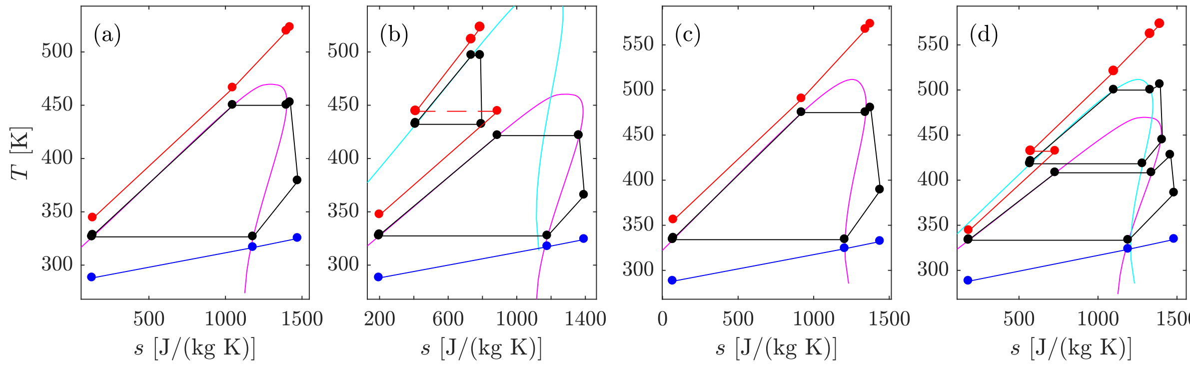

Figure 3: Optimal single-stage and cascaded systems shown on a temperature-entropy diagram: (a) 523K 1-T system; (b) 523 K 2-ST system; (c) 573 K 1-T system; and (d) 573 K 2-TT system.

4. HEAT EXCHANGER SIZING

4.1 Cross-flow evaporator sizing

The heat exchanger that transfers heat from the heat source to the working fluid is assumed to be a finned-tube cross-flow evaporator (Figure 4). This design facilitates a large heat-transfer area on the hot exhaust gas side, which has a large thermal resistance compared to the working fluid. To account for fluid property variation, and the distinct single- and two-phase regions, the heat exchanger is discretised. Each cell is a vertical slice through the heat exchanger, defined by the height and width of the frontal area, denoted H and W respectively, the number of tubes in the direction perpendicular to the flow N_{H}, and the number of columns within the cell $N_{\mathrm{L},i}$ (where $N_{\mathrm{L}} = \sum_i N_{\mathrm{L},i}$). To initialise the model an estimate for the number of columns is required, $N_{\mathrm{L},0}$, which is found from a single calculation for each of the preheating, evaporation and superheating regions. It follows that $N_{\mathrm{L},i} = N_{\mathrm{L},0}/n$, where n is the target discretisation number. For each cell, the ε-NTU method for a mixed cross-flow heat exchanger is used to determine the outlet temperatures. This process is iterative since the heat-transfer coefficients for the working fluid and heat source, denoted α_w and α_h respectively, are calculated using the mean fluid properties. For the working fluid, the Dittus-Boelter and Chen (1966) correlations are used to calculate the single- and two-phase heat-transfer coefficients respectively. Single-phase pressure drop is calculated using the Petukhov friction factor, whilst for two-phase pressure drop the correlation proposed by Muller-Steinhagen and Heck (1986) is applied. For the heat source the correlations available within the VDI Heat Atlas are applied for the heat-transfer coefficient (Schmidt, 2010) and pressure drop (Gaddis, 2010) for a bank of finned tubes. The developed model is similar to the one proposed by Kaya et al. (2015).

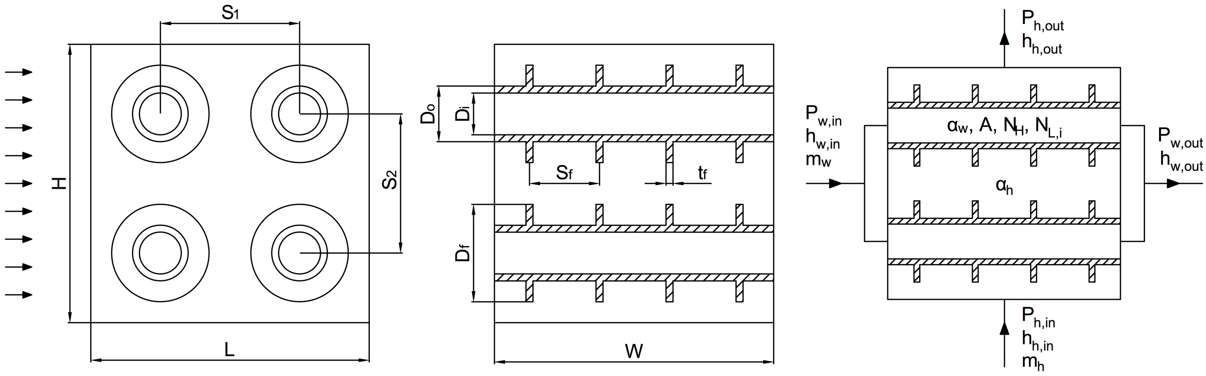

Figure 4: Simplified schematic of the the cross-flow evaporator. From left to right: side view; frontal view and description of a single discretised cell.

Referring to Figure 4, there are a number of heat-exchanger design parameters, which results in a significant computation time if they are all considered optimisation variables. For simplification, the assumptions listed in Table 3 are made, which reduces the optimisation process to one involving two design variables, namely the velocity of the incoming heat source V_h, and the pipe inner diameter D_i. Thus, the objective is to optimise these two variables to minimise the heat-transfer area subject to imposed pressure drop constraints. For the cascaded systems, an integrated evaporator is proposed (Figure 1). For these systems, it is assumed that the inner pipe diameter for the bottoming and topping cycle tubes are the same and the optimisation objective is to minimise the total combined area, subject to pressure drop constraints for the two working fluids, and a heat-source pressure drop constraint for the entire evaporator.

Table 3: Fixed geometrical parameters for the cross-flow evaporator.

Parameter	Value	Comment
W/H	1.0	Frontal area is square, hence $W = H = \sqrt{\dot{m}_h/(\rho V)_h}$
S_1/D_o	2.0	Space between pipes is equal to pipe outer diameter
S_1/S_2	1.0	Tubes are equally spaced in both directions
D_f/S_1	0.9	A value < 1 ensures fins do not interfere with fins of adjacent tubes
t_w	2 mm	Tube wall thickness
k_w	16 W/(m K)	Wall thermal conductivity; stainless steel
t_f/t_w	0.5	Fin thickness is half the tube wall thickness
S_f/t_f	5.0	Ratio of fin spacing to fin thickness

4.2 Double-pipe heat exchanger sizing

The heat exchanger used to reject heat to the cooling water, and the intermediate heat exchanger, are assumed to be double-pipe heat exchangers. Double-pipe heat exchangers are generally considered to be cost effective for small-scale applications, and since these processes predominantly involve either liquid or two-phase fluids, compact designs can be obtained. The heat-transfer areas are calculated using a discretised sizing methodology based on the log-mean temperature difference. This is defined as:

$$A = \sum_{i=1}^{n} \frac{\dot{Q}_i}{U_i \Delta T_{\log,i}}, \tag{3}$$

where n is the number of elements, and $\dot{Q}_i$, U_i and $\Delta T_{\log,i}$ are the heat-transfer rate, overall heat-transfer coefficient and counter-flow log-mean temperature difference for the i^{th} element respectively. The inner pipe is assumed to have the same wall thickness and thermal conductivity as the cross-flow evaporator (*i.e.*, t_w = 2 mm and k_w = 16 W/(m K)), whilst the optimisation variables are the pipe inner diameters. The Dittus-Boelter, Chen (1966) and Shah (1979) correlations are applied to calculate the heat-transfer coefficient for single-phase, evaporation and condensation heat-transfer, whilst the single- and two-phase pressure drops are calculated using the Petukhov friction factor and Muller-Steinhagen and Heck (1986) correlation respectively. For the condenser the working fluid passes through the inner tube. For the intermediate heat exchanger, the high-pressure evaporating fluid passes through the inner tube.

4.3 Sizing results

The results from the sizing optimisation are reported in Figure 5. For this study the maximum permissible pressure drop for the heat source and heat sink are set to 5% (*i.e.*, 5 kPa). For the single-stage systems, this same value is applied for the working fluid within the evaporator and condenser. This leads to an estimated power output reduction below 3.5%, 2.7% and 1.7% for the 473, 523 and 573 K single-stage systems respectively. For the cascaded systems a 5% pressure drop within each heat-addition and heat-rejection processes could lead to reductions in power output of 10.7%, 8.0% and 6.7% for the 473, 523 and 573 K systems respectively. Therefore the maximum possible pressure drops for these processes are reduced to 2%, which corresponds to power output reductions that are less than 4.2%, 3.1% and 2.6% respectively; these values are in-line with those estimated for the single-stage systems. For the bottoming-cycle heat addition processes within the cascaded systems, it is assumed that this 2% pressure drop is divided equally across the cross-flow evaporator and intermediate heat exchanger sections.

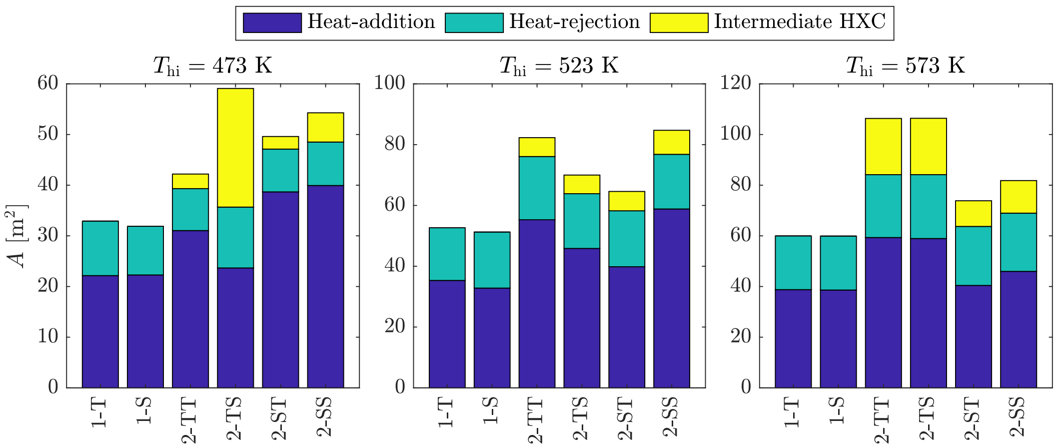

Figure 5: Total heat-transfer area required for each cycle and heat-source temperature.

It is observed that all cascaded cycles require more heat-transfer area than the single-stage systems, although the contribution from the intermediate heat exchanger is relatively low. Therefore, although this additional heat exchanger is introduced into the overall system, and that the temperature difference within this heat exchanger is low, its introduction does not have a significant affect on the required heat-transfer area. This is observed since phase-change processes are synonymous with high heat-transfer coefficients, which facilitates compact heat exchangers to be designed. The larger heat-transfer area requirements for the 2-TT and 2-TS systems is the result of having a turboexpander in the topping cycle, which leads to superheated expander outlet conditions in the topping cycle, and possibly at the expander inlet of the bottoming cycle (i.e., Figure 3(d)). This leads to vapour-to-vapour heat transfer within the intermediate heat exchanger. Comparatively, for the cascaded systems there is an increase in the area required for the heat-addition processes. This is partly attributed to the reduced exergy loss, which is synonymous with smaller temperature differences, particularly for the preheating stages (i.e., Figures 3(b) and 3(d)). However, the increase can also be associated with the tighter pressure drop constraint applied to the cascaded systems. The condenser area requirements do not vary significantly.

The change in the total heat-transfer area when moving from a 1-T system to the other systems is summarised in Figure 6. Neglecting the 473 K heat source, for which the 1-T system produces the largest power output, the 2-ST cycles result in the lowest relative increase in heat-transfer area. More specifically, the relative increases in total heat-transfer area for the 523 K and 573 K systems are 22.7% and 23.2% respectively. These two systems correspond to increases in the net power output of 4.0% and 5.9% respectively, and are two of the best performing systems. Thus, 2-ST systems may represent the most viable cascaded solution. To investigate the trade-off between the power output and heat-transfer area in more detail, suitable component cost correlations should be introduced, and a multi-objective optimisation completed. Heat-exchanger pressure drop should also be integrated into the thermodynamic analysis, removing the need to specify different pressure drop constraints for the different systems.

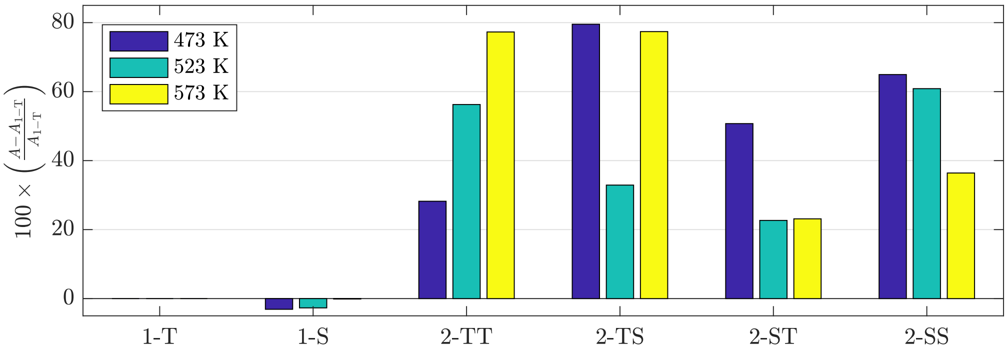

Figure 6: Total heat-transfer area required for each cycle and heat-source temperature shown relative to the area required for the single-stage system operating with a turbine (1-T).

5. CONCLUSIONS

Single-stage and cascaded ORC systems for waste-heat recovery from 473, 523 and 573 K heat sources have been compared in terms of the exergy destruction within the system, and the heat-transfer area requirements. This has provided further useful insights beyond those obtained from a previous thermodynamic comparison. The analysis reveals that the exergy destruction during the combined expansion processes in cascaded systems is between 19% and 37% less than equivalent single-stage systems. Moreover, whilst there is an exergy loss introduced by the additional heat exchange process, this is relatively small owing to the low temperature difference between the two working fluids. Cascaded cycles also reduce exergy destruction since the amount of heat transferred during evaporation is reduced. It is also found that, for cascaded cycles with two-phase expansion in the topping cycle, the intermediate heat exchanger contributes to a small portion of the total heat-transfer area. However, an increase in the heat-transfer area for the evaporator is observed, due to the reduced exergy destruction. Overall, for the 473 K heat source, a single-stage system remains the optimal solution. However, for the 523 and 573 K heat sources, a cascaded system with two-phase expansion in the topping cycle results in 4.0% and 5.9% more power, but requires 22.7% and 23.2% more heat-transfer area, compared to a single-stage system.

NOMENCLATURE

A	heat-transfer area	(m^2)
D	pipe diameter	(m)
e	specific exergy	(J/kg)
h	enthalpy	(J/kg)
$\dot{I}$	exergy destruction	(W)
$\dot{m}$	mass-flow rate	(kg/s)

P	pressure	(Pa)
$\dot{Q}$	heat-transfer rate	(W)
s	entropy	(J/kg K)
T	temperature	(K)
U	overall heat-transfer coefficient	(W/m^{2}K)
V	velocity	(m/s)
$\Delta T_{\log}$	log-mean temperature difference	(K)
α	heat-transfer coefficient	(W/m^{2}K)

Subscript

0	dead state
h	heat source
in	inlet
out	outlet
w	working fluid

REFERENCES

Chen, J. C. (1966). Correlation for boiling heat transfer to saturated fluids in convective flow. *Ind Eng Chem Proc DD*, 5(3):322–329.

Gaddis, E. S. (2010). L1.4 Pressure Drop of Tube Bundles in Cross Flow. In *VDI Heat Atlas*, pages 1076–1091. Spinger-Verlag Berline Heidelberg, 2nd edition.

Kane, M. (2003). Small hybrid solar power system. *Energy*, 28(14):1427–1443.

Kaya, A., Lazova, M., and Paepe, M. D. (2015). Design and rating of an evaporator for waste heat recovery organic Rankine cycle using SES36. In *Proceedings of the 3rd International Seminar on ORC Power Systems*, pages 1–10, 12-14 October, Brussels, Belgium.

Kosmadakis, G., Manolakos, D., Kyritsis, S., and Papadakis, G. (2009). Economic assessment of a two-stage solar organic Rankine cycle for reverse osmosis desalination. *Renew Energ*, 34(6):1579–1586.

Lecompte, S., Ameel, B., Ziviani, D., Van Den Broek, M., and De Paepe, M. (2014). Exergy analysis of zeotropic mixtures as working fluids in organic Rankine cycles. *Energ Convers Manage*, 85:727–739.

Muller-Steinhagen, H. and Heck, K. (1986). A simple friction pressure drop correlation for two-phase flow in pipes. *Chem Eng Process*, 20(6):297–308.

Read, M. G., Smith, I. K., and Stosic, N. (2017). Optimisation of power generation cycles using saturated liquid expansion to maximise heat recovery. *P I Mech Eng E-J Pro*, 23(1):57–69.

Schmidt, K. G. (2010). M1 Heat Transfer to Finned Tubes. In *VDI Heat Atlas*, pages 1273–1277. Spinger-Verlag Berline Heidelberg, 2nd edition.

Shah, M. M. (1979). A general correlation for heat transfer during film condensation inside pipes. *Int J Heat Mass Tran*, 22(4):547–556.

Smith, I. K. (1993). Development of the trilateral flash cycle system: Part 1: Fundamental considerations. *P I Mech Eng A-J Pow*, 207(3):179–194.

White, M., Read, M., and Sayma, A. (2018). Optimisation of cascaded organic Rankine cycle systems for high-temperature waste-heat recovery. In *31st International Conference on Efficiency, Cost, Optimization, Simulation and Environmental Impact of Energy Systems*, 17-22 June, Guimarães, Portugal.

White, M., Read, M., and Sayma, A. (2019). Comparison between single and cascaded organic Rankine cycle systems accounting for the effects of expansion volume ratio on expander performance. In *11th International Conference on Compressors and their Systems*, 9-11 September, London, UK.

ACKNOWLEDGEMENT

This work was supported by the UK Engineering and Physical Sciences Research Council (EPSRC) [grant number: EP/P009131/1].